Control of Face-to-Face $\pi-\pi$ Stacked Packing Arrangement of Anthracene Rings via Chalcogen−Chalcogen Interaction: 9,10-Bis(methylchalcogeno)anthracenes

Kenji Kobayashi,*[,†,‡] Hyuma Masu,[§] Atsuko Shuto,[†] and Kentaro Yamaguchi[§]

Department of Chemistry, Faculty of Science, Shizuoka University, 836 Ohya, Suruga-ku, Shizuoka 422-8529, Japan, PRESTO, JST, 4-1-8 Honcho Kawaguchi, Saitama 332-0012, Japan, and Faculty of Pharmaceutical Sciences at Kagawa Campus, Tokushima Bunri University, Shido, Sanuki, Kagawa 769-2193, Japan

Received August 20, 2005. Revised Manuscript Received October 10, 2005

Crystal packing structures of 9,10-dimethoxyanthracene (**1**), 9,10-bis(methylthio)anthracene (**2**), and 9,10-bis(methyltelluro)anthracene (**3**) were revealed by X-ray crystallographic analysis as models for the molecular ordering of acenes. Compound **1** is arranged in a herringbone packing motif similar to anthracene. In contrast, compound **2** is arranged by face-to-face $\pi-\pi$ stacking with S−S interactions. The anthracene columns of **2** formed by face-to-face $\pi-\pi$ stacking are parallel to each other and are linked by the S−S interactions to self-assemble into a 2-D network sheet. The resulting 2-D network sheets are packed parallel to each other in an offset manner. Compound **3** is arranged by face-to-face $\pi-\pi$ stacking with Te−Te interactions, concomitant with Te−π interactions, to produce a 2-D network sheet similar to **2**. Thus, the chalcogen−chalcogen interaction plays an important role in the face-to-face $\pi-\pi$ stacking arrangement of 9,10-bis(methylchalcogeno)anthracenes **2** and **3**. In contrast to **2**, the neighboring 2-D network sheets of **3** are packed to each other with large tilt angle (γ-motif). The self-assembling cyclophane-network structure of $\{[2(\mathbf{3})\cdot 2(Ag^+)]\cdot(NO_3^-)\}\cdot(NO_3^-)$ is also described.

Introduction

Compounds containing chalcogen atoms (S, Se, and Te) are a treasury of molecular electronics and can give rise to organic conductors,[1,2] organic semiconductors directed toward organic field-effect transistors (OFETs),[3,4] organic light-emitting diodes (OLEDs),[5] and photoconduction,[6] wherein intermolecular chalcogen−chalcogen interactions play an important role in the expression of functions. Acenes, linear fused polycyclic aromatic hydrocarbons, are also promising candidates for molecular electronics, especially OFETs.[7] Acenes, however, tend to be susceptible to herringbone packing arrangements,[8] which reduce the potential functions of acenes by half. Realization of a 2-D face-to-face $\pi-\pi$ stacked packing arrangement of acenes would produce improved OFET devices with a high hole mobility,[1a,7−9] because this molecular ordering permits good overlapping of the intermolecular $\pi-\pi$ orbitals. Thus, control of molecular orientation and arrangement (molecular ordering) is a very important subject for molecular electronics.

A full understanding of the nature of intermolecular interactions is a prerequisite for the design of semiconducting crystals. Several groups have reported on strategies for molecular design toward the face-to-face $\pi-\pi$ stacked

* To whom correspondence should be addressed. E-mail: skkobay@ipc.shizuoka.ac.jp.
† Shizuoka University.
‡ PRESTO.
§ Tokushima Bunri University.

(1) Review articles: (a) Roncali, J. *Chem. Rev.* **1997**, *97*, 173−205. (b) Tour, J. M. *Acc. Chem. Res.* **2000**, *33*, 791−804.
(2) (a) Williams, J. M.; Ferraro, J. R.; Thorn, R. J.; Carlson, K. D.; Geiser, U.; Wang, H. H.; Kini, A. M.; Whangbo, M.-H. *Organic Superconductors*; Prentice Hall: Englewood Cliffs, NJ, 1992. (b) Novoa, J. J.; Rovira, M. C.; Rovira, C.; Veciana, J.; Tarrés, J. *Adv. Mater.* **1995**, *7*, 233−237.
(3) For oligothiophenens, see: (a) Horowitz, G.; Bachet, B.; Yassar, A.; Lang, P.; Demanze, F.; Fave, J.-L.; Garnier, F. *Chem. Mater.* **1995**, *7*, 1337−1341. (b) Sirringhaus, H.; Brown, P. J.; Friend, R. H.; Nielsen, M. M.; Bechgaard, K.; Langeveld-Voss, B. M. W.; Spiering, A. J. H.; Janssen, R. A. J.; Meijer, E. W.; Herwig, P.; de Leeuw, D. M. *Nature* **1999**, *401*, 685−688. (c) Facchetti, A.; Deng, Y.; Wang, A.; Koide, Y.; Sirringhaus, H.; Marks, T. J.; Friend, R. H. *Angew. Chem., Int. Ed.* **2000**, *39*, 4547−4551. (d) Izumi, T.; Kobashi, S.; Takimiya, K.; Aso, Y.; Otsubo, T. *J. Am. Chem. Soc.* **2003**, *125*, 5286−5287. (e) Janzen, D. E.; Burand, M. W.; Ewbank, P. C.; Pappenfus, T. M.; Higuchi, H.; da Silva Filho, D. A.; Young, V. G.; Brédas, J.-L.; Mann, K. R. *J. Am. Chem. Soc.* **2004**, *126*, 15295−15308.
(4) For other sulfur-containing aromatics, see: (a) Laquindanum, J. G.; Katz, H. E.; Lovinger, A. J. *J. Am. Chem. Soc.* **1998**, *120*, 664−672. (b) Mas-Torrent, M.; Durkut, M.; Hadley, P.; Ribas, X.; Rovira, C. *J. Am. Chem. Soc.* **2004**, *126*, 984−985. (c) Takimiya, K.; Kunugi, Y.; Konda, Y.; Niihara, N.; Otsubo, T. *J. Am. Chem.* Soc. **2004**, *126*, 5084−5085.
(5) (a) Noda, T.; Shirota, Y. *J. Am. Chem. Soc.* **1998**, *120*, 9714−9715. (b) Sakamoto, Y.; Komatsu, S.; Suzuki, T. *J. Am. Chem. Soc.* **2001**, *123*, 4643−4644.
(6) Adam, D.; Schuhmacher, P.; Simmerer, J.; Häussling, L.; Siemensmeyer, K.; Etzbach, K. H.; Ringsdorf, H.; Haarer, D. *Nature* **1994**, *371*, 141−143.
(7) (a) Katz, H. E.; Bao, Z.; Gilat, S. L. *Acc. Chem. Res.* **2001**, *34*, 359−369. (b) Würthner, F. *Angew. Chem., Int. Ed.* **2001**, *40*, 1037−1039.
(8) (a) Desiraju, G. R. *Crystal Engineering: The Design of Organic Solids*; Elsevier: Amsterdam, 1989; Chapter 4. (b) Desiraju, G. R.; Gavezzotti, A. *Acta Crystallogr.* **1989**, *B45*, 473−482. (c) Holmes, D.; Kumaraswamy, S.; Matzger, A. J.; Vollhardt, K. P. C. *Chem.−Eur. J.* **1999**, *5*, 3399−3412. (d) Cornil. J.; Calbert, J. P.; Brédas, J.-L. *J. Am. Chem. Soc.* **2001**, *123*, 1250−1251. (e) Fritz, S. E.; Martin, S. M.; Frisbie, C. D.; Ward, M. D.; Toney, M. F. *J. Am. Chem. Soc.* **2004**, *126*, 4084−4085.
(9) Curtis, M. D.; Cao, J.; Kampf, J. W. *J. Am. Chem. Soc.* **2004**, *126*, 4318−4328 and references therein.

10.1021/cm051874t CCC: $30.25
Published on Web 11/22/2005

packing arrangement of acenes.[9−11] Anthony and co-workers reported that the introduction of a relatively bulky alkynyl group into pentacene at the 6,13-positions changes the packing structure from a herringbone motif to a face-to-face $\pi-\pi$ stacking motif.[11] Bao and co-workers reported that the introduction of halogen groups into tetracene at the 5,11-positions is effective for the control of face-to-face $\pi-\pi$ stacking,[10i] as Sarma and Desiraju pointed out that halogen groups promote π-stacking.[10a] It is known that the n$-\sigma^*$ orbital interaction between chalcogen atoms contributes to control of molecular ordering in the solid state[12] and supramolecular association in solution.[13] As a part of our projects aimed at control of molecular ordering in the solid state,[14] we report here the crystal packing structures of 9,10-bis(methylchalcogeno)anthracenes as a model for the molecular ordering of acenes,[15] wherein chalcogen−chalcogen interaction plays an important role in the face-to-face $\pi-\pi$ stacking arrangement of 9,10-bis(methylthio)anthracene (**2**) and 9,10-bis(methyltelluro)anthracene (**3**). The self-assembling cyclophane-network structure of {[2(**3**)·2(Ag^+)]·(NO_3^-)}·(NO_3^-) is also described.

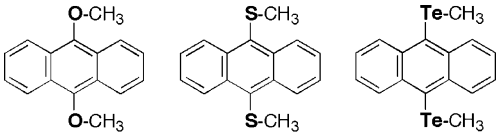

1 **2** **3**

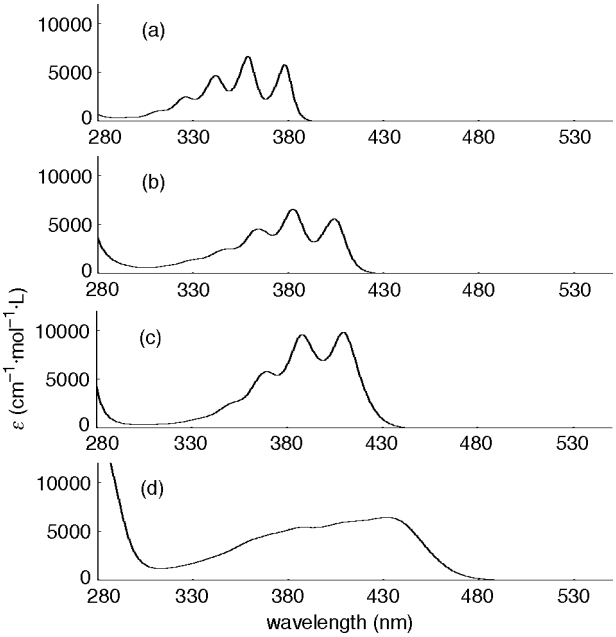

Figure 1. UV−vis spectra of (a) anthracene, (b) **1**, (c) **2**, and (d) **3** in $CHCl_3$.

Results and Discussion

Synthesis and UV−Vis Spectra. 9,10-Dimethoxyanthracene (**1**) was synthesized according to the literature.[16] 9,10-Bis(methyltelluro)anthracene (**3**) was synthesized by Engman's procedure.[17] 9,10-Bis(methylthio)anthracene (**2**)[17] was prepared by the reaction of 9,10-dilithioanthracene with dimethyl disulfide. Experimental details are shown in the Supporting Information.

UV−vis spectra of anthracene and **1**−**3** in $CHCl_3$ are shown in Figure 1. The absorption maxima of these compounds are red-shifted in the order anthracene (378 nm) < **1** (404 nm) < **2** (409 nm) < **3** (432 nm). This result suggests that the introduction of heavier chalcogen atoms into the anthracene ring decreases the HOMO−LUMO band gap. The absorption bands of **3** are highly broad compared to **1** and **2**.

Crystal Structures of 9,10-Bis(methylchalcogeno)anthracenes. Single crystals of **1**−**3** were obtained by slow evaporation of a solution of these compounds in $CHCl_3$−MeCN. Slow evaporation of a solution of a 1:1 mixture of **3** and $AgNO_3$ in $CHCl_3$−MeCN gave single crystals of **3**·$AgNO_3$·$0.5H_2O$. In contrast, a 1:1 mixture of **2** and $AgNO_3$ under the same conditions produced single crystals of **2** alone. X-ray crystallographic analyses of these single crystals revealed their packing structures, which are described in the following sections. All crystallographic data are summarized in Table 1. The ORTEP views indicate that the side chains of **1**−**3** show the *anti*-conformation, whereas that of **3**·$AgNO_3$ exhibits the *syn*-conformation (Figure S1).

Crystal Packing Structure of 9,10-Dimethoxyanthracene (1). It is well-known that the packing structure of anthracene adopts a herringbone packing motif.[8b,18] Compound **1** is also arranged in a herringbone packing motif without any

(10) (a) Sarma, J. A. R. P.; Desiraju, G. R. *Acc. Chem. Res.* **1986**, *19*, 222−228. (b) Herwig, P. T.; Müllen, K. *Adv. Mater.* **1999**, *11*, 480−483. (c) Meng, H.; Bendikov, M.; Mitchell, G.; Helgeson, R.; Wudl, F.; Bao, Z.; Siegrist, T.; Kloc, C.; Chen, C.-H. *Adv. Mater.* **2003**, *15*, 1090−1093. (d) Ito, K.; Suzuki, T.; Sakamoto, Y.; Kubota, D.; Inoue, Y.; Sato, F.; Tokito, S. *Angew. Chem., Int. Ed.* **2003**, *42*, 1159−1162. (e) Perepichka, D. F.; Bendikov, M.; Meng, H.; Wudl, F. *J. Am. Chem. Soc.* **2003**, *125*, 10190−10191. (f) Miao, Q.; Nguyen, T.-Q.; Someya, T.; Blanchet, G. B.; Nuckolls, C. *J. Am. Chem. Soc.* **2003**, *125*, 10284−10287. (g) Weidkamp, K. P.; Afzali, A.; Tromp, R. M.; Hamers, R. J. *J. Am. Chem. Soc.* **2004**, *126*, 12740−12741. (h) Tulevski, G. S.; Miao, Q.; Fukuto, M.; Abram, R.; Ocko, B.; Pindak, R.; Steigerwald, M. L.; Kagan, C. R.; Nuckolls, C. *J. Am. Chem. Soc.* **2004**, *126*, 15048−15050. (i) Moon, H.; Zeis, R.; Borkent, E.-J.; Besnard, C.; Lovinger, A. J.; Siegrist, T.; Kloc, C.; Bao, Z. *J. Am. Chem. Soc.* **2004**, *126*, 15322−15323.

(11) (a) Anthony, J. E.; Brooks, J. S.; Eaton, D. L.; Parkin, S. R. *J. Am. Chem. Soc.* **2001**, *123*, 9482−9483. (b) Anthony, J. E.; Eaton, D. L.; Parkin, S. R. *Org. Lett.* **2002**, *4*, 15−18. (c) Odom, S. A.; Parkin, S. R.; Anthony, J. E. *Org. Lett.* **2003**, *5*, 4245−4248. (d) Payne, M. M.; Odom, S. A.; Parkin, S. R.; Anthony, J. E. *Org. Lett.* **2004**, *6*, 3325−3328. (e) Payne, M. M.; Parkin, S. R.; Anthony, J. E.; Kuo, C.-C.; Jackson, T. N. *J. Am. Chem. Soc.* **2005**, *127*, 4986−4987.

(12) (a) Guru Row, T. N.; Parthasarathy, R. *J. Am. Chem. Soc.* **1981**, *103*, 477−479. (b) Desiraju, G. R. *Crystal Engineering: The Design of Organic Solids*; Elsevier: Amsterdam, 1989; Chapter 7. (c) Desiraju, G. R.; Nalini, V. *J. Mater. Chem.* **1991**, *1*, 201−203. (d) Werz, D. B.; Gleiter, R.; Rominger, F. *J. Am. Chem. Soc.* **2002**, *124*, 10638−10639. (e) Gleiter, R.; Werz, D. B.; Rausch, B. J. *Chem.−Eur. J.* **2003**, *9*, 2676−2683. (f) Gleiter, R.; Werz, D. B. *Chem. Lett.* **2005**, *34*, 126−131 and references therein.

(13) (a) Kobayashi, K.; Deguchi, N.; Takahashi, O.; Tanaka, K.; Horn, E.; Kikuchi, O.; Furukawa, N. *Angew. Chem., Int. Ed.* **1999**, *38*, 1638−1640. (b) Kobayashi, K.; Koyama, E.; Kono, C.; Namatame, K.; Nakamura, K.; Furukawa, N. *J. Org. Chem.* **2001**, *66*, 2085−2090. (c) Kobayashi, K.; Tanaka, K.; Izawa, H.; Arai, Y.; Furukawa, N. *Chem.−Eur. J.* **2001**, *7*, 4272−4279. (d) Kobayashi, K. *J. Synth. Org. Chem. Jpn.* **2002**, *60*, 859−868.

(14) Kobayashi, K.; Sato, A.; Sakamoto, S.; Yamaguchi, K. *J. Am. Chem. Soc.* **2003**, *125*, 3035−3045.

(15) For monolayer morphology of 1,5-bis[2-(alkylthio)ethyl]anthracenes on graphite, see: Wei, Y.; Kannappan, K.; Flynn, G. W.; Zimmt, M. B. *J. Am. Chem. Soc.* **2004**, *126*, 5318−5322.

(16) Kraus, G. A.; Man, T. O. *Synth. Commun.* **1986**, *16*, 1037−1042.

(17) Engman, L.; Hellberg, J. S. E. *J. Organomet. Chem.* **1985**, *296*, 357−366.

Table 1. Crystallographic Data for 1−3 and 3·$AgNO_3$·0.5H_2O

param	1	2	3	3·$AgNO_3$·0.5H_2O
formula	$C_{16}H_{14}O_2$	$C_{16}H_{14}S_2$	$C_{16}H_{14}Te_2$	$C_{16}H_{14}Te_2AgNO_{3.5}$
fw	238.27	270.39	461.47	639.35
cryst system	orthorhombic	triclinic	monoclinic	monoclinic
space group	*Pbca*	$P\bar{1}$	*C*2/*c*	*C*2/*c*
a (Å)	8.6048(11)	5.1950(18)	20.240(3)	23.262(4)
b (Å)	8.4436(11)	7.458(3)	5.7906(7)	10.0197(19)
c (Å)	16.095(2)	9.002(3)	15.698(2)	15.761(3)
α (deg)	90	74.066(5)	90	90
β (deg)	90	73.691(4)	129.4820(10)	94.638(3)
γ (deg)	90	89.762(5)	90	90
V (Å^3)	1169.4(3)	320.87(19)	1420.0(3)	3661.5(12)
Z	4	1	4	8
temp (K)	90	173	90	150
R_1 ($I > 2\sigma(I)$)	0.0388	0.0553	0.0226	0.0583
wR_2 (all data)	0.1041	0.1677	0.0585	0.1668
GOF	1.034	1.093	1.067	0.953
packing motif	herringbone[a]	face-to-face $\pi-\pi$ stacking	face-to-face $\pi-\pi$ stacking (*γ*-motif[a])	sandwich-herringbone[a]

[a] See ref 18.

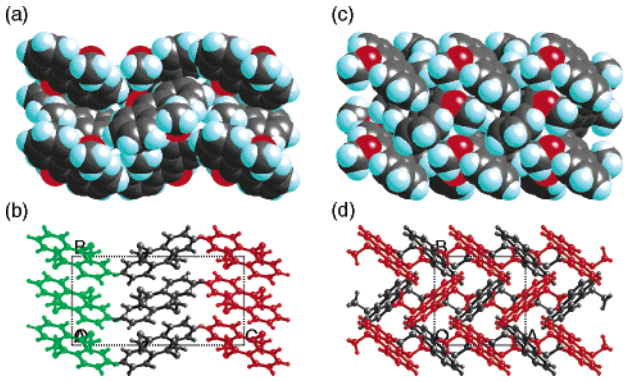

Figure 2. 3-D crystal packing structure of 9,10-dimethoxyanthracene (**1**): (a, b) view looking down the *a* axis; (c, d) side view looking down the *c* axis.

heteroatom interaction, as shown in Figure 2. The translated interplanar distance of anthracene rings along the *b* axis is 8.4436 Å (Figure 2c,d). The interplanar tilt angle between two neighboring anthracene rings is 67.2°, and the close intermolecular C···C′ contacts within 3.75 Å are C3···C2′ = 3.635 Å, C3···C7′ = 3.695 Å, C4···C6′ = 3.753 Å, and C4···C7′ = 3.592 Å. The intermolecular closest O···O′ distance is 4.236 Å, indicating no interaction between oxygen atoms.

Crystal Packing Structure of 9,10-Bis(methylthio)-anthracene (2). In marked contrast to **1**, the crystal packing structure of compound **2** reveals that **2** is aligned by face-to-face $\pi-\pi$ stacking along the *a* axis with S−S interactions, as shown in Figure 3. The details of the crystal packing structure are shown in Figures 4 and 5.

Figure 4 shows one network sheet of **2** composed of face-to-face $\pi-\pi$ stacking and S−S interactions, which are defined in Figure 3a. Figure 4a shows one network sheet looking down the *a* axis. Figure 4b,e (front view) shows one network sheet inclined to the *a* axis of Figure 4a by 41°, that is, the view looking down the long molecular axis. The intermolecular S···S′ distance in **2** is 3.638 Å. Although the S···S′ distance is almost the same as the sum of the van der Waals radii of two sulfur atoms,[19,20] this value is still in the range of van der Waals interaction.[12d,f] The contact angles of S···S′−C_{Anth} and S···S′−C_{Me} are 175.527 and 84.293°, respectively (Figure 4d). This S···S′ contact is almost coplanar across an inversion center, where two azimuthal angles are equal. One sulfur atom approaches the other sulfur atom along the σ^*(S−C_{Anth}) orbital of the other. This result indicates that this S−S interaction cannot be a n−σ^* interaction between the lone pair orbital of one sulfur atom and the σ^*(S−C) orbital of the other but is likely an isotropic van der Waals dispersion force.[12a,b,f] Thus, the S−S interaction forms the 1-D network of **2**.

Figure 4b,e (front view) and Figure 4c,f (top view) indicate that the anthracene ring of **2** forms the anthracene column through a face-to-face $\pi-\pi$ slip-stacking motif along the *a* axis,[11b] with a face-to-face anthracene−anthracene distance of 3.39 Å. The anthracene rings in one column are slipped relative to each other along the long molecular axis by 3.73

(18) Desiraju and Gavezzotti classified crystal packing structures of polycyclic aromatic hydrocarbons into four basic structure types: herringbone, sandwich-herringbone, *γ*-motif, and *β*-motif.[8a,b] Possible space groups that allow close-packing for molecules with a center of symmetry are restricted to *P*1, $P2_1/c$, $P2_1/a$, *C*2/*c*, or *Pbca*. The majority of crystal systems are monoclinic, the minority are orthorhombic, and none of the compounds adopt triclinic packing. The key parameters in separating the four structure types are the shortest cell axis and the interplanar angle, defined as the angle between the mean plane of one molecule and that of its nearest neighbors.[8a,b] *Herringbone*: CH−*π* (edge-to-face) interactions between nonparallel near neighbors are important; the shortest cell axis is between 5.4 Å and 8 Å with interplanar angles between 40 and 80°, showing a clear trend of decreasing interplanar angle with increasing short axis. Typical examples are acenes and terphenyl. *Sandwich-herringbone*: This structure type is similar to the herringbone but for the fact that the recurring motif is a diad of face-to-face $\pi-\pi$ stacked molecules (the sandwich). Above a short axis value of 8 Å, this structure type displays a trend similar to that for the herringbone type; typical examples are pyrene and perylene. *γ-Motif*: Both face-to-face $\pi-\pi$ stacking and herringbone motif are important, and infinite stacks of molecules (columns) formed by face-to-face $\pi-\pi$ stacking are close packed through CH−π (edge-to-face) interactions. This motif shows short axis values in the range 4.6−5.4 Å with large interplanar angles around 80°; typical examples are coronene and hexabenzocoronene.[22] *β-Motif*: This type is a layered structure made up of graphitic planes and is characterized by strong face-to-face $\pi-\pi$ stacking without significant contribution from CH−π interactions. This motif shows short axis values up to 4.2 Å with small interplanar angles in the range 5−30°; typical examples are tribenzopyrene and benzodicoronene.[22]

(19) (a) Bondi, A. *J. Phys. Chem.* **1964**, *68*, 441−451. (b) Pauling, L. *The Nature of the Chemical Bond*, 3rd ed.; Cornell University Press: Ithaca, NY, 1973.

(20) The sum of van der Waals radii of two atoms is as follows: S···S = 3.60 (3.70) Å; S···C = 3.50 (3.55) Å; Te···Te = 4.12 (4.40) Å; Te···C = 3.76 (3.90) Å; C···C = 3.40 (3.40) Å. The values and those in parentheses are based on refs 19a,b, respectively.

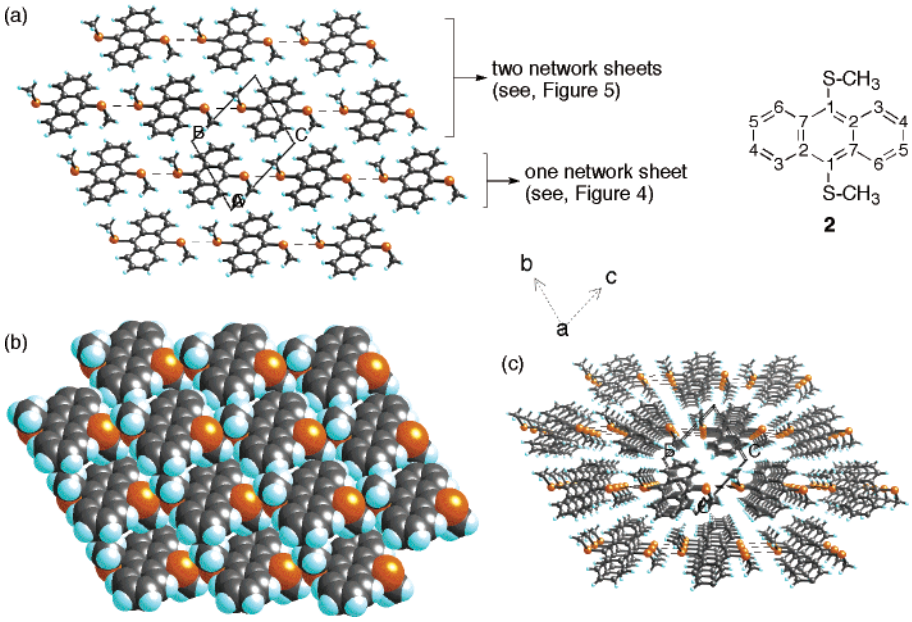

Figure 3. 3-D packing structure of 9,10-bis(methylthio)anthracene (**2**): (a) view looking down the *a* axis; (b) space-filling representation of view a; (c) perspective view of view a.

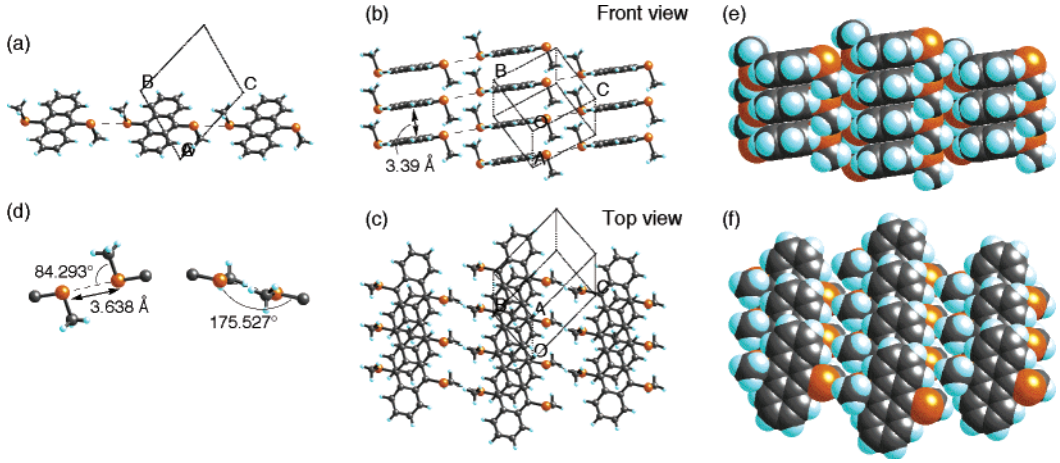

Figure 4. 2-D network sheet of **2** defined in Figure 3a: (a) view looking down the *a* axis; (b, e) front view (view looking down the long molecular axis); (c, f) top view; (d) S−S interaction.

Å and the short molecular axis by 1.28 Å. The close intermolecular C···C′ distances, within 3.65 Å, in one anthracene column are C1···C4′ = 3.501 Å, C1···C5′ = 3.454 Å, C2···C2′ = 3.641 Å, C2···C3′ = 3.505 Å, C2···C4′ = 3.601 Å, C3···C7′ = 3.454 Å, and C4···C7′ = 3.618 Å, wherein six aromatic carbons participate in the face-to-face $\pi-\pi$ slip-stacking. There may be a very weak S$-\pi$ interaction between the sulfur atom and the anthracene ring in the anthracene column, with the interatomic distances of S···C5′ = 3.609 Å and S···C6′ = 3.650 Å.[20] There is no S−S interaction (5.195 Å) within the anthracene column.

Thus, the anthracene columns of **2** formed by face-to-face $\pi-\pi$ slip-stacking are parallel to each other and are linked by the S−S interactions to self-assemble into a 2-D network sheet, wherein the direction of the S−S interaction is perpendicular to the direction of the face-to-face $\pi-\pi$ slip-stacking (Figure 4).

Figure 5 shows the correlation between two neighboring 2-D network sheets, which are colored blue and red. The neighboring 2-D network sheets are parallel to each other, as shown in Figure 5b (front view) and Figure 5d (side view). However, face-to-face $\pi-\pi$ stacking between the neighboring network sheets is scarcely observed, as shown in Figure 5c (top view). The anthracene columns in one network sheet shown in red are stacked, in an offset manner, on top of the moieties connected by the S−S interaction between the anthracene columns in the neighboring network sheet shown in blue. The close C···C′ distances between the two neighboring network sheets are C5···C6′ = 3.700 Å and C6···C6′ = 3.770 Å between column A and column B, indicating scarce overlapping of $\pi-\pi$ orbitals, and are $C8_{Me}$···C4′ = 3.553 Å and $C8_{Me}$···C5′ = 3.677 Å between column A′ and column B, undoubtedly showing CH$-\pi$ interactions.[21]

Crystal Packing Structure of 9,10-Bis(methyltelluro)-anthracene (3). Compound **3** is aligned by face-to-face $\pi-\pi$ stacking along the *b* axis with Te−Te interactions (Figure 6). The anthracene columns of **3** formed by face-to-face $\pi-\pi$

(21) All columns are identical structures, although columns A and A′ belong to one network sheet and columns B and B′ belong to the neighboring network sheet.

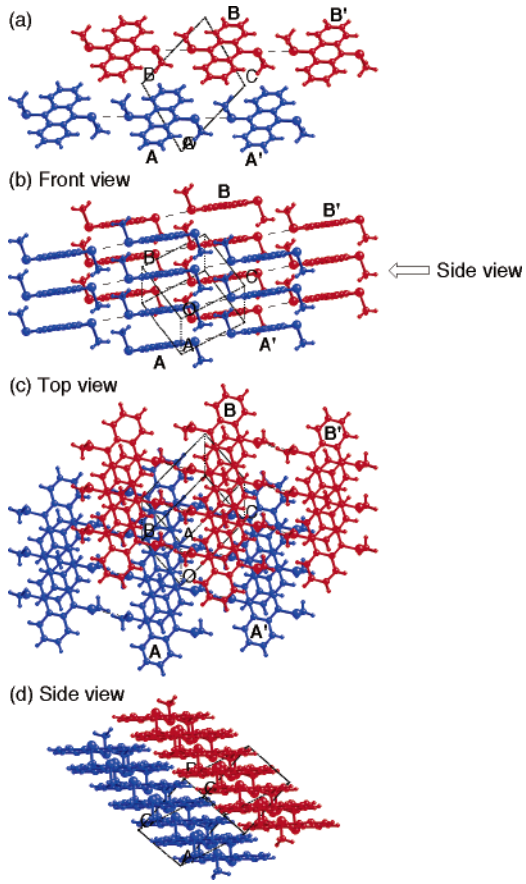

Figure 5. Packing structure of two neighboring 2-D network sheets of **2** shown in blue and red: (a) view looking down the *a* axis; (b) front view (view looking down the long molecular axis); (c) top view; (d) side view.

slip-stacking are parallel to each other and are linked by the Te−Te interactions to self-assemble into a 2-D network sheet like compound **2**. However, the 3-D crystal packing structure of **3** shown in Figure 6 is different from that of **2** in the following two aspects: (1) Te−π interactions evidently exist in each anthracene column. (2) The neighboring 2-D network sheets are packed to each other with large tilt angle. The details of the crystal packing structure of **3** are shown in Figures 7 and 8.

Figure 7 shows one network sheet of **3** composed of face-to-face $\pi-\pi$ stacking and Te−Te interactions, which are defined in Figure 6a. Figure 7a,c (front view) shows one network sheet inclined to the *b* axis of Figure 6a by 38°, that is, the view looking down the long molecular axis. The intermolecular Te···Te′ distance in **3** is 3.747 Å, which is obviously shorter than the sum of the van der Waals radii of two tellurium atoms.[20] The contact angles of Te···Te′−C_{Anth} and Te···Te′−C_{Me} are 149.068 and 84.676°, respectively (Figure 7e). This Te···Te′ contact is symmetrical owing to the presence of an inversion center between the two tellurium atoms. One tellurium atom approaches the other tellurium atom nearly along the σ^*(Te−C_{Anth}) orbital of the other. This result indicates that this Te−Te interaction can be explained in terms of isotropic van der Waals dispersion force rather than as an n−σ^* interaction.[12a,b,f] Thus, the Te−Te interaction forms the 1-D network of **3**.

Figure 7a,c (front view) and Figure 7b,d (top view) indicate that the anthracene ring of **3** forms the anthracene column through a face-to-face $\pi-\pi$ slip-stacking motif along the *b* axis,[11b] with a face-to-face anthracene−anthracene distance of 3.46 Å. The anthracene rings in one column are slipped relative to each other along the long molecular axis by 4.19 Å and the short molecular axis by 2.05 Å. The close intermolecular C···C′ distances, within 3.70 Å, in one anthracene column are C1···C6′ = 3.555 Å, C2···C7′ = 3.535 Å, C2···C6′ = 3.621 Å, and C7···C7′ = 3.691 Å, wherein four aromatic carbons participate in the face-to-face $\pi-\pi$ slip-stacking.

In the anthracene column of **3**, Te−π interactions between the tellurium atom and the anthracene ring undoubtedly exist along the *b* axis (Figure 7a,c), together with the face-to-face $\pi-\pi$ slip-stacking, with contact distances of Te···C5′ = 3.539 Å and Te···C4′ = 3.777 Å and contact angles of Me−Te···C5′ = 165.537° and Me−Te···C4′ = 172.700°. These contact distances are significantly shorter than the sum of the van der Waals radii of tellurium and aromatic carbon atoms.[20] There is no Te−Te interaction (5.791 Å) within the anthracene column. The Te−π interaction in the anthracene column of **3** is much more effective than S−π interaction of **2** probably to compensate that the overlapping of intermolecular $\pi-\pi$ orbitals in the anthracene column of **3** is not greater than that of **2** (vide infra).

Thus, the anthracene columns of **3** formed by face-to-face $\pi-\pi$ slip-stacking and Te−π interactions are parallel to each other and are linked by the Te−Te interactions to self-assemble into a 2-D network sheet, wherein the direction of the Te−Te interaction is perpendicular to the direction of the face-to-face $\pi-\pi$ slip-stacking and Te−π interaction (Figure 7).

Figure 8 shows the correlation between two neighboring 2-D network sheets, which are colored blue and red. The neighboring 2-D network sheets are identical structures and are packed to each other with a large tilt angle. The anthracene columns in one network sheet shown in blue are placed, in an offset manner, on top of the moieties connected by the Te−Te interaction between the anthracene columns in the neighboring network sheet shown in red, as shown in Figure 8b,e (front view) and Figure 8c (top view). The tilt angle between the two neighboring network sheets is 75.9°, as shown in Figure 8d,f (side view). The close C···C′ distances between the two neighboring network sheets are C4···C5′ = 3.519 Å, C4···C6′ = 3.644 Å, and C5···C5′ = 3.705 Å.

One of the reasons for the difference in the packing structure of neighboring 2-D network sheets in **3** from that in **2** would be attributed to the difference in efficiency of chalcogen−π interactions between chalcogen atom and anthracene ring in the column. The value of (interatomic distance between two atoms)/(sum of van der Waals radii of two atoms) may be one of the factors indicating the efficiency of these interactions. In the cases of both chalcogen−chalcogen interaction between columns and chalcogen−π interaction in the column, values in **3** are smaller than those in **2** (Table 2); namely, both interactions in **3** are greater than those in **2**. The stronger Te−π interaction in **3** would enhance the slipping of the face-to-face $\pi-\pi$ stacking of anthracene rings as compared to the weaker S−π

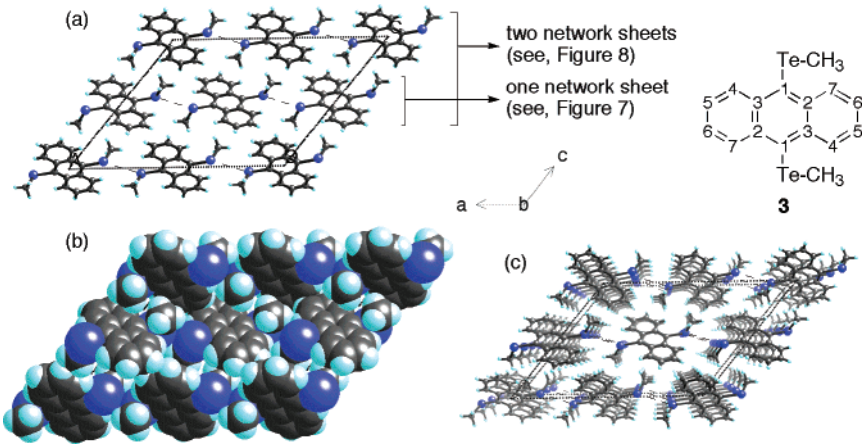

Figure 6. 3-D packing structure of 9,10-bis(methyltelluro)anthracene (**3**): (a) view looking down the *b* axis; (b) space-filling representation of view a; (c) perspective view of view a.

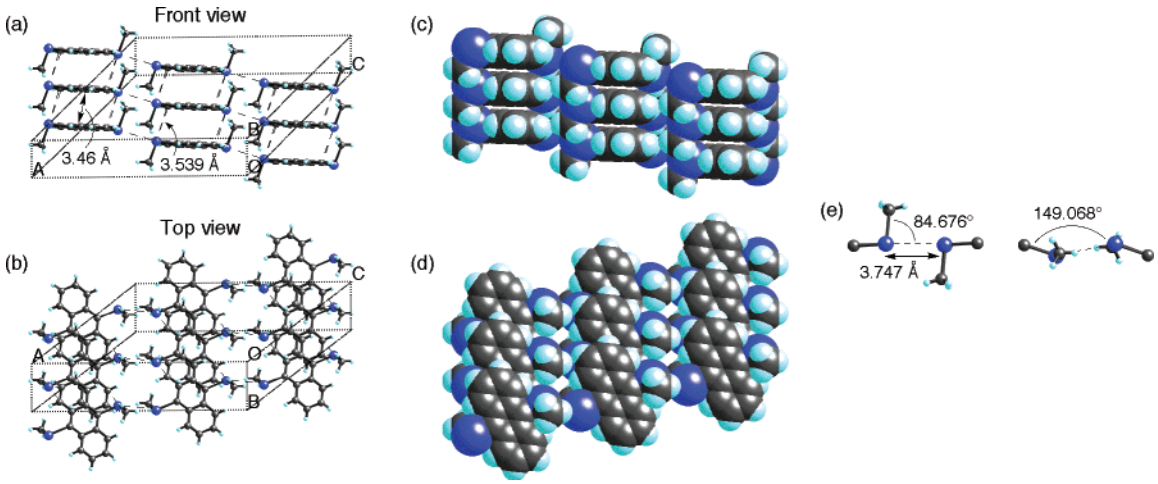

Figure 7. 2-D network sheet of **3** defined in Figure 6a: (a, c) front view (view looking down the long molecular axis); (b, d) top view; (e) Te−Te interaction.

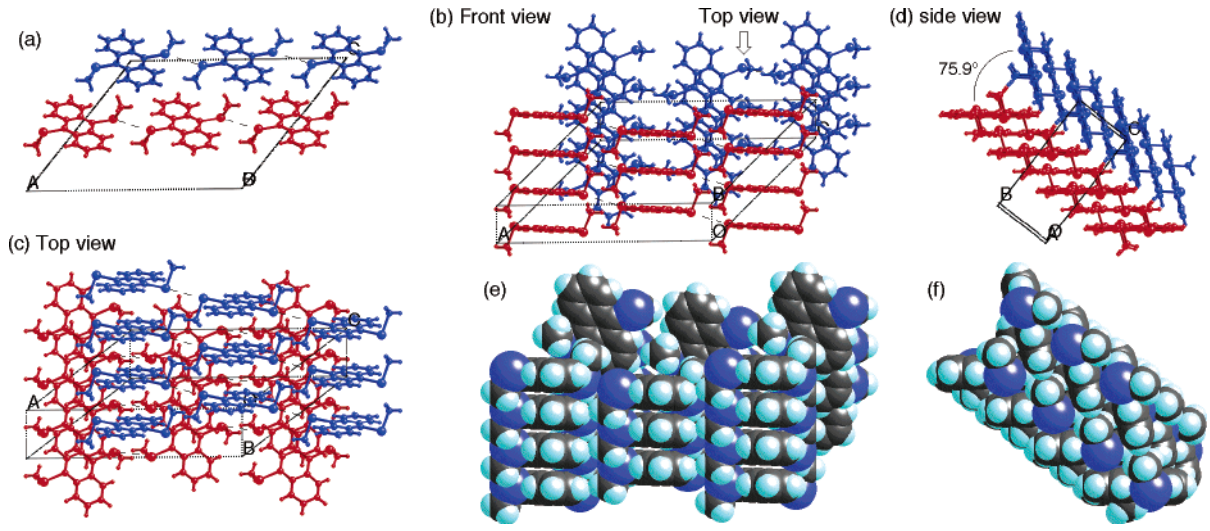

Figure 8. Packing structure of two neighboring 2-D network sheets of **3** shown in blue and red: (a) view looking down the *b* axis; (b, e) front view (inclined to the *b* axis of view a by 38°); (c) top view; (d, f) side view.

interaction in **2**. The relatively large slip of anthracene rings in the column of **3** would give rise to a herringbone-like packing arrangement with large tilt angle between the neighboring 2-D network sheets. The 3-D packing structure of **3** belongs to a γ-motif, which is defined by Desiraju and Gavezzotti.[8a,b,18,22]

1:1 Complex of 9,10-Bis(methyltelluro)anthracene (3) with $AgNO_3$. Compound **3** coordinates with $AgNO_3$ to give a 1:1 complex, $\{[2(\mathbf{3})\cdot 2(Ag^+)]\cdot(NO_3^-)\}\cdot(NO_3^-)\cdot 0.5H_2O$.[23] As a basic unit, two molecules of **3** and two Ag^+ assemble into

(22) Goddard, R.; Haenel, M. W.; Herndon, W. C.; Krüger, C.; Zander, M. *J. Am. Chem. Soc.* **1995**, *117*, 30−41.

Table 2. Values of (Interatomic Distance between Two Atoms)/(Sum of van der Waals Radii of Two Atoms) and Slip Distances in the Face-to-Face $\pi-\pi$ Stacking

param	**2** (X = *S*-Me)	**3** (X = *Te*-Me)	**3**·$AgNO_3$·0.5H_2O (X = *Te*-Me)
(X···X)/vdW(X···X)[a]	1.012 (0.983)	0.909 (0.852)	0.988 (0.925)
($X\cdots C_{Ant}$)/vdW	1.031; 1.043	0.941; 1.004	
($X\cdots C_{Ant}$)[a]	(1.017; 1.028)	(0.907; 0.968)	
slip dist (Å)			
long axis[b]	3.73	4.19	2.95
short axis[c]	1.28	2.05	0.80

[a] Values and those in parenthses are based on Bondi's and Pauling's data, respectively.[19,20] [b] Slip along the long molecular axis. [c] Slip along the short molecular axis.

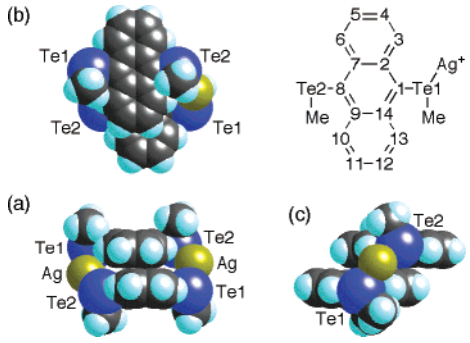

Figure 9. Cyclophane unit of **3**·$AgNO_3$·0.5H_2O: (a) front view; (b) top view; (c) side view.

a cyclophane [2(**3**)·2(Ag^+)] mediated by Te−Ag coordination bonds with distances of Te1−Ag = 2.703 Å and Te2−Ag = 2.740 Å, as shown in Figure 9.[24] The coordination bond angles are Te1−Ag−Te2 = 135.941°, C1−Te1−Ag = 96.598°, and C8−Te2−Ag = 114.149°. The two anthracene rings in the cyclophane experience face-to-face $\pi-\pi$ stacking with a face-to-face anthracene−anthracene distance of 3.30 Å and are moderately slipped relative to each other along the long molecular axis by 2.95 Å and the short molecular axis by 0.80 Å. This is the maximal face-to-face overlapping of anthracene rings among the packing structures studied in this paper (Table 2). The close intermolecular C···C′ distances, within 3.65 Å, in the cyclophane are C1···C10′ = 3.625 Å, C2···C11′ = 3.488 Å, C7···C11′ = 3.429 Å, C7···C12′ = 3.486 Å, C8···C12′ = 3.442 Å, C8···C13′ = 3.562 Å, C9···C9′ = 3.590 Å, C9···C14′ = 3.633 Å, and C10···C14′ = 3.510 Å, wherein 10 aromatic carbons participate in the face-to-face $\pi-\pi$ stacking.

Two kinds of NO_3^- coordinate to Ag^+ of the cyclophane [2(**3**)·2(Ag^+)], as shown in Figure 10e.[23] One NO_3^- (N2, O3−5) serves as a monodentate ligand with the Ag−O3 distance of 2.441 Å. The other NO_3^- (N1, O1, O2) serves as a bidentate ligand with the Ag−O1 = 2.421 Å, which is linked to the cyclophanes to give a 1-D coordination cyclophane-network of $\{\{[2(\mathbf{3})\cdot 2(Ag^+)]\cdot(NO_3^-)\}\cdot(NO_3^-)\}_n$, as shown in Figure 10a−d. The coordination angles around Ag^+ are Te1−Ag−Te2 = 135.941°, Te1−Ag−O3 = 97.296°,

(23) The occupancy factors of two kinds of NO_3^- are 0.5 and 0.5, respectively.

(24) For a cyclophane and its network assembled by the coordination of chalcogen compounds with silver ions, see: (a) Dai, J.; Kuroda-Sowa, T.; Munakata, M.; Maekawa, M.; Suenaga, Y.; Ohno, Y. *J. Chem. Soc., Dalton Trans.* **1997**, 2363−2368. (b) Shimizu, G. K. H.; Enright, G. D.; Ratcliffe, C. I.; Ripmeester, J. A. *Chem. Commun.* **1999**, 461−462.

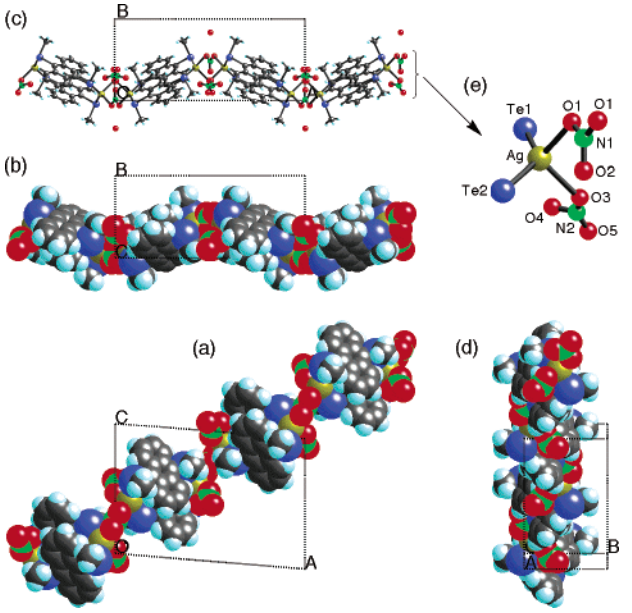

Figure 10. 1-D coordination cyclophane network of **3**·$AgNO_3$·0.5H_2O:[23] (a) front view looking down the *b* axis; (b, c) top view looking down the *c* axis; (d) side view looking down the *bc* plane; (e) coordination geometry of Ag^+ in **3**·$AgNO_3$·0.5H_2O. In views a, b, and d, H_2O molecules as an inclusion solvent are omitted for clarity.

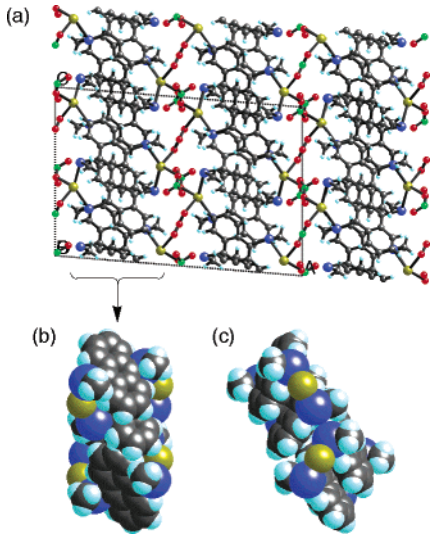

Figure 11. 3-D packing structure of **3**·$AgNO_3$·0.5H_2O: (a, b) front view looking down the *b* axis; (c) side view of view b.

Te2−Ag−O3 = 108.605°, Te1−Ag−O1 = 112.241°, Te2−Ag−O1 = 94.554°, and O3−Ag−O1 = 105.792°, indicating a distorted tetrahedral coordination geometry of Ag^+ (Figure 10e). Figure 11a shows the 3-D packing structure of $\{[2(\mathbf{3})\cdot 2(Ag^+)]\cdot(NO_3^-)\}\cdot(NO_3^-)\cdot 0.5H_2O$. The neighboring 1-D coordination networks of $\{\{[2(\mathbf{3})\cdot 2(Ag^+)]\cdot(NO_3^-)\}\cdot(NO_3^-)\}_n$ are packed to each other by a herringbone arrangement of cyclophane moieties, together with a weak Te−Te interaction of Te1···Te2 = 4.072 Å, as shown in Figure 11b,c. In the herringbone packing of cyclophane moieties between neighboring 1-D coordination networks, the close intermolecular C···C′ distances within 3.75 Å are C5···C9′ = 3.666 Å, C5···C14′ = 3.699 Å, C12···C5′ = 3.743 Å, and C12···C6′ = 3.703 Å. Thus, the 3-D packing structure of **3**·$AgNO_3$·0.5H_2O belongs to a typical sandwich-herringbone motif.[8a,b,18]

Conclusion

We have demonstrated that the chalcogen−chalcogen interaction plays an important role in the face-to-face $\pi-\pi$ stacking arrangement of 9,10-bis(methylthio)anthracene (**2**) and 9,10-bis(methyltelluro)anthracene (**3**), whereas 9,10-dimethoxyanthracene (**1**) is arranged in a herringbone packing motif similar to anthracene.

The anthracene columns of **2** formed by face-to-face $\pi-\pi$ slip-stacking were parallel to each other and were linked by S−S interactions to self-assemble into a 2-D network sheet, wherein the direction of the S−S interaction was perpendicular to the direction of the face-to-face $\pi-\pi$ slip-stacking. In the 3-D packing structure, the neighboring 2-D network sheets were parallel to each other in an offset manner, and significant overlapping of $\pi-\pi$ orbitals between the neighboring network sheets was scarcely observed.

In similar to **2**, the anthracene columns of **3** formed by face-to-face $\pi-\pi$ slip-stacking and Te−π interactions were parallel to each other and were linked by the Te−Te interactions to self-assemble into a 2-D network sheet, wherein the direction of the Te−Te interaction was perpendicular to the direction of the face-to-face $\pi-\pi$ slip-stacking and Te−π interaction. In contrast to **2**, the neighboring 2-D network sheets of **3** were packed to each other with large tilt angle (γ-motif),[8a,b,18] probably due to the relatively large slipping of the anthracene rings in the column caused by the Te−π interaction.

In the complex of **3**·$AgNO_3$, the cyclophanes [2(**3**)·2(Ag^+)], which were formed by Te−Ag coordination bonds, were linked by NO_3^- to give a 1-D coordination cyclophane network of $\{\{[2(\mathbf{3})\cdot 2(Ag^+)]\cdot(NO_3^-)\}\cdot(NO_3^-)\}_n$. The packing structure showed a sandwich-herringbone motif[8a,b,18] between cyclophanes in neighboring 1-D coordination networks.

The results presented here suggest that the introduction of methylchalcogeno groups into acenes and the use of chalcogen−chalcogen interaction may provide a new approach to molecular design for the control of face-to-face $\pi-\pi$ stacked packing arrangements of acenes.[9−11] The synthesis of 6,13-bis(alkylchalcogeno)pentacenes directed toward OFETs is underway in our laboratory.

Supporting Information Available: Synthetic procedures and spectral data for **1**−**3** and ORTEP views of **1**−**3** and **3**·$AgNO_3$·$0.5H_2O$ and their X-ray experimental details in the form of a crystallographic information file (CIF). This material is available free of charge via the Internet at http://pubs.acs.org.

CM051874T